Physical characteristics of localized surface plasmons resulting from nano-scale structured multi-layer thin films deposited on D-shaped optical fiber

T. Allsop,[1,*] R. Neal,[2] M. Dvorak,[3] K. Kalli,[4] A. Rozhin,[1] D.J. Webb[1]

[1]*Aston Institute of Photonic Technologies, Aston University, Aston Triangle, Birmingham, B47ET, UK*
[2]*Dept of Maths and Computing, Faculty of Science and Technology, University of Plymouth, Plymouth, PL4 8AA, UK*
[3]*Institute of Physical Engineering/CEITEC, Brno University of Technology, Technická 2/10, Brno 616 69, Czech Republic*
[4]*Cyprus University of Technology, 31 Archbishop Kyprianos, Lemessos 3036, Cyprus*
**t.d.p.allsop@aston.ac.uk*

Abstract: Novel surface plasmonic optical fiber sensors have been fabricated using multiple coatings deposited on a lapped section of a single mode fiber. UV laser irradiation processing with a phase mask produces a nano-scaled surface relief grating structure resembling nano-wires. The resulting individual corrugations produced by material compaction are approximately 20 μm long with an average width at half maximum of 100 nm and generate localized surface plasmons. Experimental data are presented that show changes in the spectral characteristics after UV processing, coupled with an overall increase in the sensitivity of the devices to surrounding refractive index. Evidence is presented that there is an optimum UV dosage (48 joules) over which no significant additional optical change is observed. The devices are characterized with regards to change in refractive index, where significantly high spectral sensitivities in the aqueous index regime are found, ranging up to 4000 nm/RIU for wavelength and 800 dB/RIU for intensity.

OCIS codes: (240.6680) Surface plasmons; (060.2370) Fiber optics sensors; (220.4241) Nanostructure fabrication; (280.4788) Optical sensing and sensors.

References and links

1. E. Kretschmann, "Decay of non-radiative surface plasmons into light on rough silver films: Comparison of experimental and theoretical results," Opt. Commun. **6**(2), 185–187 (1972).
2. C. Nylander, B. Liedberg, and T. Lind, "Gas detection by means of surface plasmon resonance," Sens. Actuators **3**, 79–88 (1982).
3. T Allsop, R. Neal, S. Rehman, C. Zhang, D. J. Webb, D. Mapps, and I. Bennion, "Surface Plasmon Resonance Generation Utilising Gratings for Biochemical Sensing," OFS-18 Cancun Mexico, paper WA4, (2006).
4. J. M. Brockman, B. P. Nelson, and R. M. Corn, "Surface Plasmon Resonance Imaging Measurements of Ultra-thin Organic Films," Annu. Rev. Phys. Chem. **51**(1), 41–63 (2000).
5. R. Karlsson and A. Fält, "Experimental design for kinetic analysis of protein-protein interactions with surface plasmon resonance biosensors," J. Immunol. Methods **200**(1-2), 121–133 (1997).
6. J. Homola, "Present and future of surface plasmon resonance biosensors," Anal. Bioanal. Chem. **377**(3), 528–539 (2003).
7. X. D. Hoa, A. G. Kirk, and M. Tabrizian, "Towards integrated and sensitive surface plasmon resonance biosensors: a review of recent progress," Biosens. Bioelectron. **23**(2), 151–160 (2007).
8. H. Raether, *Surface Plasmons on Smooth and Rough Surfaces and on Grating* (Academic, 1997)
9. T. Allsop, R. Neal, S. Rehman, D. J. Webb, D. Mapps, and I. Bennion, "Generation of infrared surface plasmon resonances with high refractive index sensitivity utilizing tilted fiber Bragg gratings," Appl. Opt. **46**(22), 5456–5460 (2007).
10. A. J. Haes and R. P. Van Duyne, "A unified view of propagating and localized surface plasmon resonance biosensors," Anal. Bioanal. Chem. **379**(7-8), 920–930 (2004).
11. T. Arai, P. K. R. Kumar, C. Rockstuhl, K. Awazu, and J. Tominaga, "An optical biosensor based on localized surface plasmon resonance of silver nanostructured films," J. Opt. A, Pure Appl. Opt. **9**(7), 699–703 (2007).

#189539 - $15.00 USD Received 30 Apr 2013; revised 14 Jul 2013; accepted 21 Jul 2013; published 31 Jul 2013

12. J. Y. Chyan, C. A. Chang, and J. A. Yeh, "Development and characterization of a broad-bandwidth polarization-insensitive sub-wavelength optical device," Nanotechnology **17**(1), 40–44 (2006).
13. T. Allsop, R. Neal, C. Mou, K. Kalli, S. Saied, S. Rehman, D. J. Webb, P. F. Culverhouse, J. L. Sullivan, and I. Bennion, "Formation and characterisation of ultra-sensitive surface plasmon resonance sensor based upon a nano-scale corrugated multi-layered coated D-shaped optical fibre," J. Quantum Electron. **48**(3), 394–405 (2012).
14. M. Piliarik, J. Homola, Z. Manıková, and J. Čtyroký, "Surface plasmon resonance sensor based on a single-mode polarisation-maintaining optical fiber," Sens. Actuators B Chem. **90**, 236–242 (2004).
15. X. Fan, I. M. White, S. I. Shopova, H. Zhu, J. D. Suter, and Y. Sun, "Sensitive optical biosensors for unlabeled targets: A review," Anal. Chim. Acta **620**(1-2), 8–26 (2008).
16. C. Genet and T. W. Ebbesen, "Light in tiny holes," Nature **445**(7123), 39–46 (2007).
17. E. Hutter, J. Eliza, and J. H. Fendler, "Exploitation of localized surface plasmon resonance," Adv. Mater. **16**(19), 1685–1706 (2004).
18. D. C. Skigin and M. Lester, "Study of resonant modes of a periodic metallic array near a dielectric interface: evanescent-to-propagating coupling via surface plasmon excitation," J. Opt. A, Pure Appl. Opt. **8**(3), 259–267 (2006).
19. S. O. Kucheyev, J. R. Hayes, J. Biener, T. Huser, C. E. Talley, and A. V. Hamza, "Surface-enhanced Raman scattering on nanoporous Au," Appl. Phys. Lett. **89**(5), 053102 (2006).
20. D. L. Williams, S. T. Davey, R. Kashyap, J. R. Armitageand, and B. J. Ainslie, "UV spectroscopy of optical fibres and performs," Proc. Soc. Photo Opt. Instrum. Eng. **1516**, 29 (1991).
21. D. Gonbeau, V. Pamukchieva, R. Dedryvere, E. Skordeva, and D. Arsova, "Photoinduced changes in the valence band states $Ge_XAs_{40-X}S_{60}$ of thin films," J. Optoelectron. Adv. Mater. **7**(1), 341–344 (2005).
22. M. M. Miller and A. A. Lazarides, "Sensitivity of Metal Nanoparticle Surface Plasmon Resonance to the Dielectric Environment," J. Phys. Chem. B **109**(46), 21556–21565 (2005).
23. K.-S. Lee and M. A. El-Sayed, "Gold and Silver Nanoparticles in Sensing and Imaging: Sensitivity of Plasmon Response to Size, Shape, and Metal Composition," J. Phys. Chem. B **110**(39), 19220–19225 (2006).
24. A. G. Brolo, R. Gordon, B. Leathem, and K. L. Kavanagh, "Surface plasmon sensor based on the enhanced light transmission through arrays of nanoholes in gold films," Langmuir **20**(12), 4813–4815 (2004).

1. Introduction

Surface plasmon resonance (SPR) has been investigated since the mid-twentieth century using bulk optical components, in particular using the Ottoman Kretschmann apparatus [1]. In the 1980's researchers used for the first time SPR as a sensing platform [2] and over the last two decades there has been increased interest in the potential applications of SPR in the fields of chemistry, biochemistry and biology [3–7] due to its high spectral sensitivity to changes in refractive index. Surface plasmon resonance is an optical phenomenon that involves a resonant transfer of incident propagating light energy to a surface-plasmon mode that takes the form of collective electron oscillations at the interface between a metal and a dielectric material [8]. The majority of the work undertaken in the past relates to two specific types of surface plasmons: the long range surface plasmon (LRSP) [4] and the short range surface plasmon (SRSP) [9]. More recently interest has turned to another type of plasmon, the localised surface plasmon (LSP) [10] following advances in technology to produce structured thin films that have nano-scaled periodic or quasi-periodic surfaces [10–13]. It is well known that SPR generation is very sensitive to the polarization of the illuminating light, its wavelength and its angle of incidence on the metal surface. The polarisation sensitivity can be used to detect index changes in biochemical/chemical reactions [14]. SPR biosensors offer the opportunity for real-time and label-free monitoring of biomolecular interactions [15].

The plasmons exist at a metal–dielectric interface with a dispersion relationship that depends on the topology of the supporting metal coating [8]. It is known that both LRSP and SRSP obey the following dispersion relation for two homogeneous semi-infinite media:

$$\beta = k\sqrt{\left(\frac{\varepsilon_m \cdot n_s^2}{\varepsilon_m + n_s^2}\right)} \tag{1}$$

where k is the free space wave number, ε_m is the dielectric constant of the metal ($\varepsilon_m = \varepsilon_{mr} + i\,\varepsilon_{mi}$) and n_s is the refractive index of the dielectric sample to be tested. A periodically structured surface consisting of metal and dielectric materials (a corrugated nano-structure) can be considered as an array of apertures in the supporting surface plasmon material [16],

#189539 - $15.00 USD Received 30 Apr 2013; revised 14 Jul 2013; accepted 21 Jul 2013; published 31 Jul 2013

with momentum component of light parallel to the surface $k_x = \frac{2\pi}{p} \cdot \sqrt{i^2 + j^2}$, where p is a lattice constant (the distance between the apertures), i and j are nonzero integers representing the scattering orders from the two dimensional aperture array with the suffix x referring to a direction perpendicular to the row of apertures. The resonant condition for the localized surface plasmons that needs to be satisfied for such a lattice structure is given by reference 16. Localized surface plasmons (LSP) display a more complex behavior than LRSP as there are several dependencies, for example on the size, topology and geometries of the plasmon-supporting nanostructures. Examples of the effects of surface topology on the spectral behavior of plasmons can easily be found in the literature [10]. The optical properties and characteristics of structured thin film can be comprehensively tuned by nano-engineering the structure parameters, such as using periodically arranged nanopores or microporous and nanoporous metal structures [10, 17–19].

There is a considerable body of published research relating to optical fibre devices for refractive index sensing [15] with SPR fiber optic sensors being one of the types being investigated [6] due to their high spectral sensitivity to refractive index change in the aqueous index regime [12].

We report on the fabrication and characterization of SPR fiber devices that use a lapped, D-shaped single-mode optical fiber on which is deposited multiple thin film layers of materials consisting of metals, semiconductors and oxides. We have shown previously, evidence that the device behavior results from a coupling mechanism between the fiber core mode and localized surface plasmons [13]. In this paper we provide experimental data of the changing spectral transmission characteristics of the fiber during the generation of nano-scale surface relief corrugation as part of the fabrication process. We show typical topologies produced during the UV processing that creates these structures. The experimental data also indicate that the optimum UV energy dosage does not depend on the type of metal overlay coating. We demonstrate that the spectral sensitivity to refractive index after UV processing increases approximately 2 orders of magnitude. Finally we illustrate the polarization dependence of these devices and that the plasmon resonances can be tuned using polarization over a wavelength range from the visible to 2 μm.

2. Fabrication and structuring of thin film stacks on the optical fiber

The fiber devices were processed in three stages. Firstly, a standard single mode fiber (Corning, SMF-28e) was mechanically lapped to within 6μm of the core-cladding interface. Secondly, vacuum RF plasma sputtering was used to deposit a series of three thin film coatings onto the flat region of the lapped fiber. The materials used for these coatings were firstly germanium (48nm) followed by silicon dioxide (48nm) and finally either gold, silver or platinum (32nm) an illustration of how the multi-layered coatings are constructed is show in Fig. 1. The various thicknesses were estimated by means of a witness plate. The coated fiber (length of 2.2cm) was exposed to a UV light interference pattern produced with a uniform phase mask of period 1.018μm, using multiple exposures of the UV laser (Innova® Sabre® FRED), operating at 244nm and scanned along the fiber with a scanning velocity of 0.05mms^{-1} and with UV optical powers on the fiber of from 106mW up to 265mW. Some experimental data describing the overall changes that occur during these three processes have been presented in earlier work [13]. The result of these three process stages is the formation of long thin strips of metal along the peaks (nano-wires/nano-rods) and insulation material in the grooves. Here we are concerned with investigating the last process; the generation of the nano-scale surface relief corrugation, illustrated by the experimental data shown in Figs. 2 and 3. The spectral sensitivity to refractive index and polarization of the transmission spectral features of the fiber devices are investigated before, during and after formation of this structure. Figure 1 shows the experimental set-up used for polarization characterization both during fabrication and when the fiber devices are submerged into various liquids with different refractive indices. Light from a broadband light source was passed through a

#189539 - $15.00 USD Received 30 Apr 2013; revised 14 Jul 2013; accepted 21 Jul 2013; published 31 Jul 2013

polarizer and a polarization controller before illuminating the sample, with the transmission spectrum being monitored using an optical spectrum analyzer. The change in polarization of the illuminating light was monitored with a polarimeter (Tektronix, PAT 9000B) through a polarization maintaining coupler, see Fig. 1.

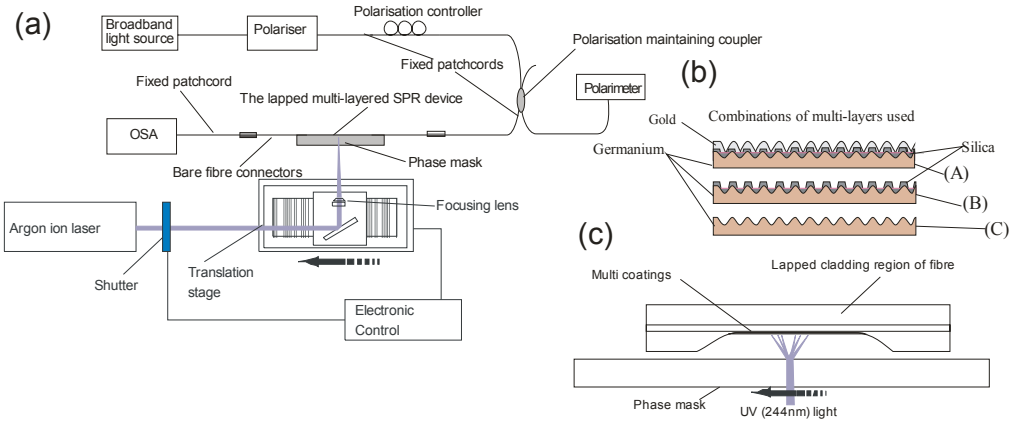

Fig. 1. **(a)** Scheme used for the characterization of the devices, (b) representation of the construction of UV processed coating (c) schematic of the alignment of coated D-shaped fiber.

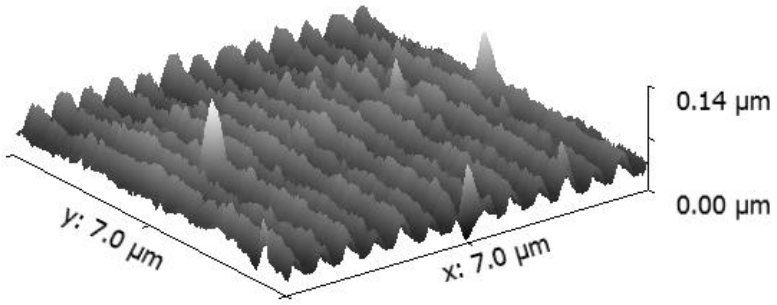

Fig. 2. A three dimensional view showing the surface topology of the flat of the D-shaped, platinum coated device obtained using AFM.

Inspecting Figs. 2 and 3, firstly it may be seen from the data obtained using atomic force microscopy (AFM) that the corrugations are uniform. This is illustrated by performing a Fast Fourier Transform (FFT) on the AFM data, which shows a uniform sinusoid with a predominant spatial frequency of 0.526 µm, see Fig. 4. The overall length of the individual corrugations is approximately 20 µm with an average FWHM of 100 ± 20 nm, thus the length of the uniform perturbation is approximately 2 orders of magnitude greater in size than the width, therefore approaching the metal nano-wire regime. Inspecting Figs. 3(c) and 3(d) shows that the general height of these structures is 35 ± 10 nm, which is the thickness of the metal overlay and thus these nano-wires are surrounded by dielectric materials comprising the supporting SiO_2 layer beneath the metal layer and the surrounding environment elsewhere.

#189539 - $15.00 USD Received 30 Apr 2013; revised 14 Jul 2013; accepted 21 Jul 2013; published 31 Jul 2013

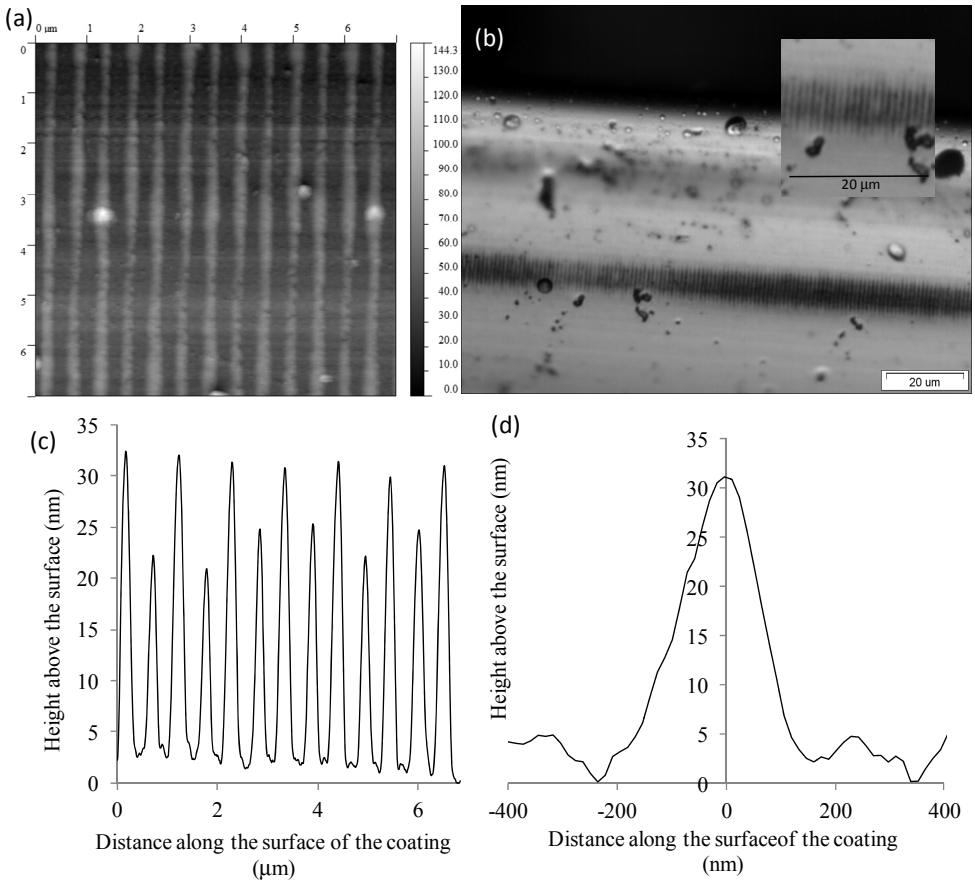

Fig. 3. Images and topological data of the post UV-laser processed platinum device: (a) an AFM image; (b) a visible microscope image with a magnified insert; (c) a line profile across the surface of the device; (d) a typical profile of a single corrugation.

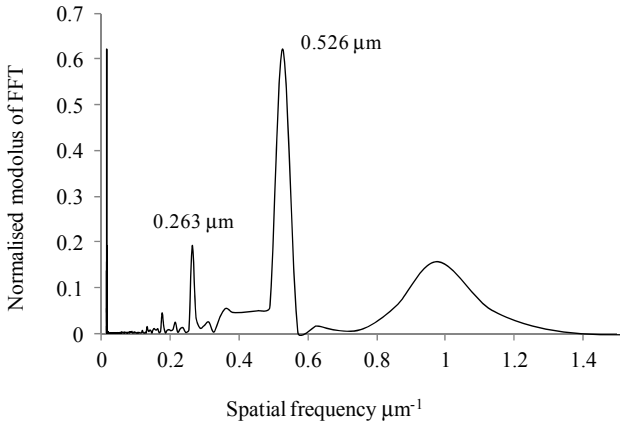

Fig. 4. A fast Fourier transform (FFT) of the typical AFM line profile of the post-UV processed multi-layered fiber.

It is understood from previous work [13] that the UV processing creates a surface corrugation that induces a strain gradient into the D-shaped optical fiber [13]. The details of

#189539 - $15.00 USD Received 30 Apr 2013; revised 14 Jul 2013; accepted 21 Jul 2013; published 31 Jul 2013

the production of the surface relief modulation that occurs in the coating during UV light exposure is still under investigation, however it is well known that UV illumination is responsible for photo-bleaching and compaction of Ge/GeO_2 doped materials such as doped glasses [20]. We envisage that spatially periodic UV illumination of the Ge and SiO_2 layers in our device produces a surface corrugation due to this compaction. X-ray photoelectron spectroscopy (XPS) is a quantitative spectroscopic technique that analyses the surface of a material, measuring the elemental composition and chemical state of the elements that exist in the surface region by determining the binding energies of the electrons. This technique was used to investigate the coating material and detected the presence of germanium oxides which are known to produce the structural change in the material [13, 21]. We suggest that the compaction associated with the surface corrugation creates a quasi-periodic strain field in the coating and the fiber substrate that extends into the core, which then acts to couple light from the core into the surface plasmon mode.

The magnitude of this strain field determines the coupling strength to the SPR. It can be concluded that, given the limited amount of Ge and SO_2 (and thus the germanium oxides response for structural compaction) that is deposited within the coating, there would be a limit on possible compaction available regardless of the length UV exposure (i.e. energy dosage). Thus, with the same coating thickness of Ge and SiO_2 (regardless of the metal overlay) the same net effect with UV exposure should be observed. The UV exposure process will result in a change in the spectral locations of the resonances for the surface plasmons due to the compaction in the material and the change in the physical characteristics of the coating. It is this change in the surface structure that causes the conventional LRSP to no longer be supported, with localized surface plasmons instead being generated

To support the above viewpoint, the spectral characteristics of the SPR excitation features of the fiber devices were monitored during fabrication. Typically, new strong spectral features would appear, see Fig. 5(a) suggesting different physical mechanism. The procedure to record these spectral features is to slightly vary the azimuthal polarization after each scan to maximize the strength of the feature under scrutiny. Analysing the results suggests there appears to be an asymptotic behavior for the observed spectral changes as a function of UV energy exposure, supporting the suggestion of limited change available described above. This asymptotic behavior can be seen by inspecting the wavelength shift and mean optical strength of the main spectral transmission features; see Figs. 5(b) and 5(c) as well as Fig. 6, where the effect is clearer. Beyond approximately 48 joules of UV energy, there are no more significant changes in the transmission profile of the fiber devices. The noise and spectral artifacts exhibited in the transmission spectra Fig. 5(a) is due to the detection limits of the optical spectrum analyzer and associated broadband light source.

#189539 - $15.00 USD Received 30 Apr 2013; revised 14 Jul 2013; accepted 21 Jul 2013; published 31 Jul 2013

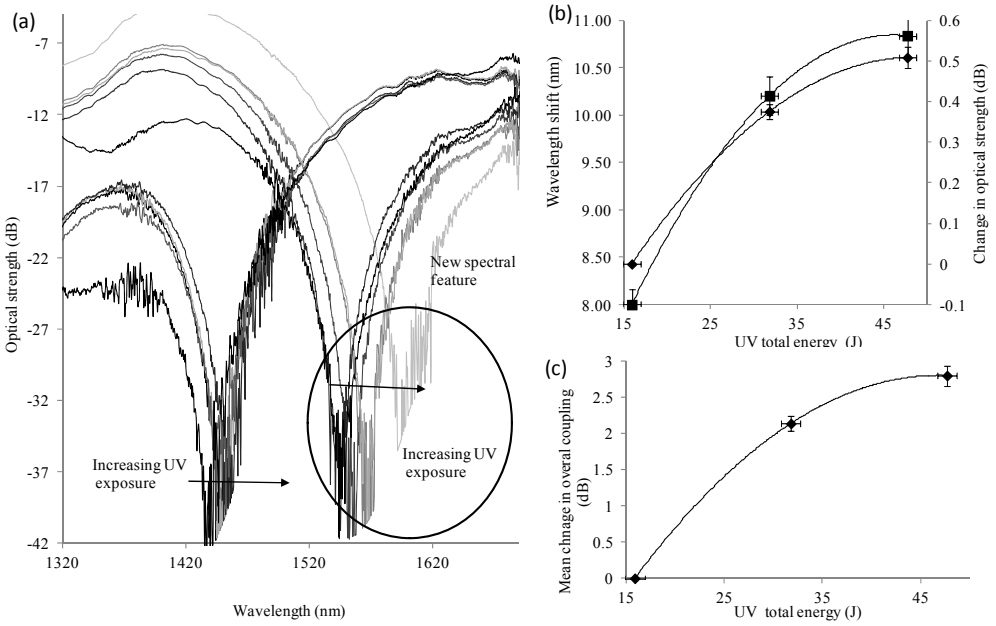

Fig. 5. (a) The observed spectral changes of the Pt-SPR fiber device during UV processing. (b) The spectral behavior of the predominant spectral features as a function of the UV energy delivered to the fiber. (c) The change in background coupling after each UV exposure.

The spectral characteristics of the SPR devices as a function of energy dosage have been studied for different metal overlay coatings; Fig. 6 shows results obtained using Au and Ag. These other metal devices showed similar optical behavior to the platinum device shown in Fig. 5.

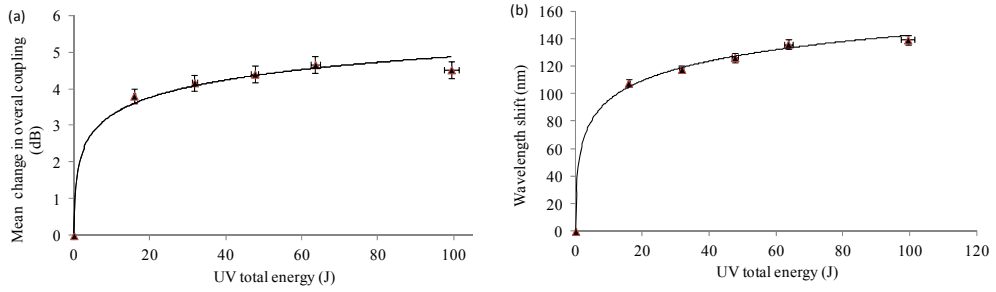

Fig. 6. The spectral behavior of the predominant spectral features as a function of the UV energy delivered to the gold coated device. (a) The mean change in coupling after each UV exposure. (b) The wavelength shift of the centroid of the main spectral feature.

This spectral behavior seen with platinum (Fig. 5) and gold (Fig. 6) has also been observed with a silver metal over-coating. Thus with the same coating thickness of Ge and SiO_2 (regardless of the metal overlay) the same net effect with UV exposure is observed.

2. Optical characterization and surface topology of the optical fiber devices

The spectral sensitivity of the SPR devices to environmental parameters after UV exposure is enhanced compared to before the processing. Some typical experimental results that show this enhanced behavior are presented in Figs. 7 and 8 (Pt-SiO_2-Ge fiber device, with thicknesses 34nm, 48nm, 48nm respectively). The noise exhibited in the transmission spectra in Fig. 8(a) is due to the detection limitations of the optical spectrum analyzer operating with the

#189539 - $15.00 USD Received 30 Apr 2013; revised 14 Jul 2013; accepted 21 Jul 2013; published 31 Jul 2013

associated light source over this wavelength range. Strong optical excitations of the plasmons' resonances were found in the spectral range 1200nm to 1700nm with the strongest resonance shifting in wavelength following exposure: e.g. 1370nm before processing and 1550nm afterwards. Similar results were found for gold and silver coated devices. The silver metal overlay coated fiber device yielded a wavelength spectral sensitivity of $d\lambda/dn$ = 4000 nm/RIU and an intensity spectral sensitivity of dI/dn = 800 dB/RIU in the aqueous index regime after UV processing compared to values of $d\lambda/dn$ = 600 nm/RIU for wavelength and a value of dI/dn = 120 dB/RIU for intensity before UV processing.

Another example of this enhanced sensitivity comes from a gold metal over-coated SPR fiber device (Au-SiO_2-Ge fiber device, with thicknesses 34nm, 48nm, 48nm respectively), which yielded an initial spectral sensitivity (before UV exposure) of dI/dn = 7.5 ± 0.3 dB/RIU and $d\lambda/dn$ = 33.7 ± 0.5 nm/RIU, while after the UV processing it became dI/dn = 135.0 ± 0.5 dB/RIU and $d\lambda/dn$ = –280.2 ± 0.4 nm/RIU; these results show over an order of magnitude increase in spectral sensitivity of the sensor to changes in surrounding refractive index in the aqueous index regime. Secondly, the main spectral feature occurs at a different wavelength after UV processing; this suggests from the theory of SPR [8] that the coating topology has changed and/or the overall thickness has changed. Effectively the UV process transforms the initially planar surface supporting conventional surface plasmons into effectively an array of metallic nano-rods lying along the tops of the surface grooves. Such a structure supports localized surface plasmons that have different resonance conditions and different dispersive properties which accounts for the increased sensitivity and its different sign for wavelength shift. It was also observed that plasmon resonances could be found over a large wavelength range by changing the polarization state of the illuminating light.

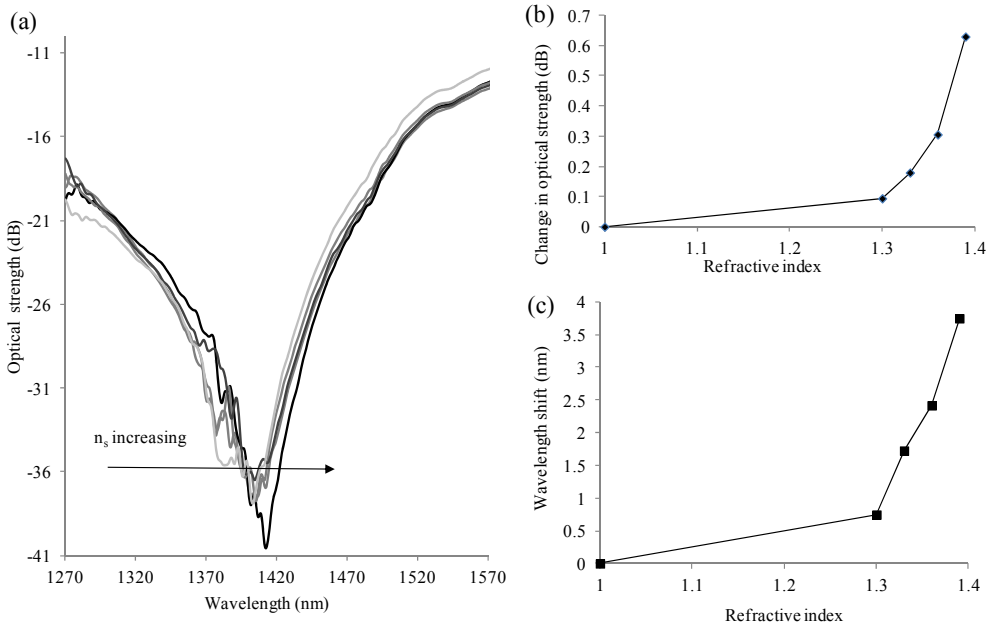

Fig. 7. (a) The spectral transmission profiles for increasing index of the surrounding medium. The spectral characteristics of the Pt-SiO_2-Ge SPR fiber device as a function of index prior to UV processing: (b) change in optical strength and (c) shift in central wavelength of the spectral feature.

#189539 - $15.00 USD Received 30 Apr 2013; revised 14 Jul 2013; accepted 21 Jul 2013; published 31 Jul 2013

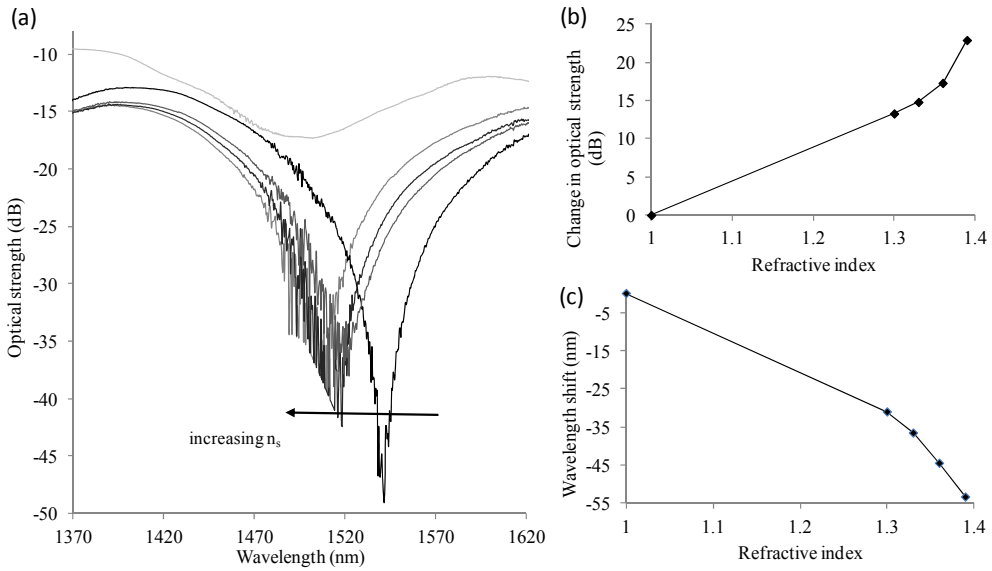

Fig. 8. (a) The spectral transmission profiles for increasing index of the surrounding medium. The spectral characteristics of the UV-processed Pt-SiO_2-Ge SPR fiber device as a function of index: (b) change in optical strength and (c) shift in central wavelength of the spectral feature.

Using part of the apparatus shown in Fig. 1 it was possible to investigate the polarization properties of these devices. Before UV processing there are two spectral features at 1320nm and 1650nm that can be varied in optical strength from 0dBm to −15dBm but not in wavelength by changing the azimuthal polarization of the illuminating light. After UV processing, the first observation is that many more LSP resonances exist and they can be tuned over an extremely broad wavelength range from 1000nm to 2000nm, depending upon the metal overlay used. This spectral tuning ability is shown in Fig. 9(a) and Fig. 9(b) for platinum and gold by varying the polarization state of the illuminating light.

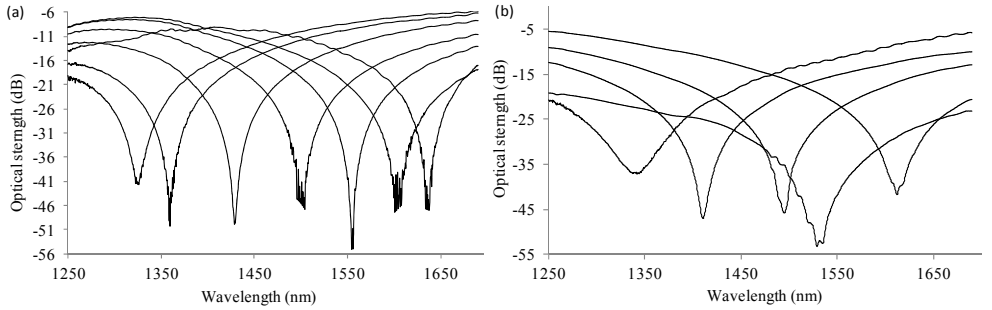

Fig. 9. The observed surface plasmon resonances obtained at different wavelengths by varying polarization state of the illuminating light for the device consisting of (a) Pt-SiO_2-Ge and (b) Au-SiO_2-Ge, both with a surrounding refractive index of 1.36.

A more detailed study of the plasmon's resonances as a function of azimuthal polarization of the illuminating light was made before and after UV processing. A typical response of a gold metal overlay coating is shown in Fig. 10. Firstly, this tunability behavior is expected and has been observed previously and relates to surface roughness of the coating [9]. Secondly, there is an overall increase in sensitivity to change in the azimuthal polarization, from −0.167 dB degree^{-1} to −1.2 dB degree^{-1} after UV processing. Thirdly, there is an overall reduction in the spectral tunability for a given resonance condition as a function of the change in azimuthal polarization state. By way of illustrating this experimental observation, we note

#189539 - $15.00 USD Received 30 Apr 2013; revised 14 Jul 2013; accepted 21 Jul 2013; published 31 Jul 2013

that the gold metal overlay fiber device's wavelength range of significant strength of excitation reduces from 60° before UV processing to 20° and a significantly less wavelength range after UV processing. Similar spectral behavior was also observed with metal overlay coatings of silver and platinum and a summary of typical results is shown in Table 1. This kind of spectral behavior is expected when physical surface attributes are changed from a uniform and singular material with a flat planar surface to a non-uniform and complex material composition with varying topology. Initially the devices have a coating, the surface of which has enough roughness to cause the surface plasmons to be damped, having a short propagation length and having a large wavelength tunability [9] as a function of azumuthal polarization, as seen in Fig. 10(a). After UV processing the coating is transformed into a corrugated surface topology (and can be considered as rods of metal with nano-scale dimensions) where the surface plasmons become localized and the polarization tunability [22] becomes shape dependent, as seen in Fig. 10(b). This sensitivity does not depend on the type of the metal but depends largely on the aspect ratio of the nano-rods being formed. The direct dependence of the sensitivity on the aspect ratio becomes more prominent as the size of the nano-rods becomes larger [23] which is observed with silver and platinum coated devices. Thirdly, there is an increase in the insertion loss of the devices which has been discussed previously [13]. Furthermore this UV-induced change in the surface topology results in different spectral resonances and changes the spectral sensitivity to environmental measurands.

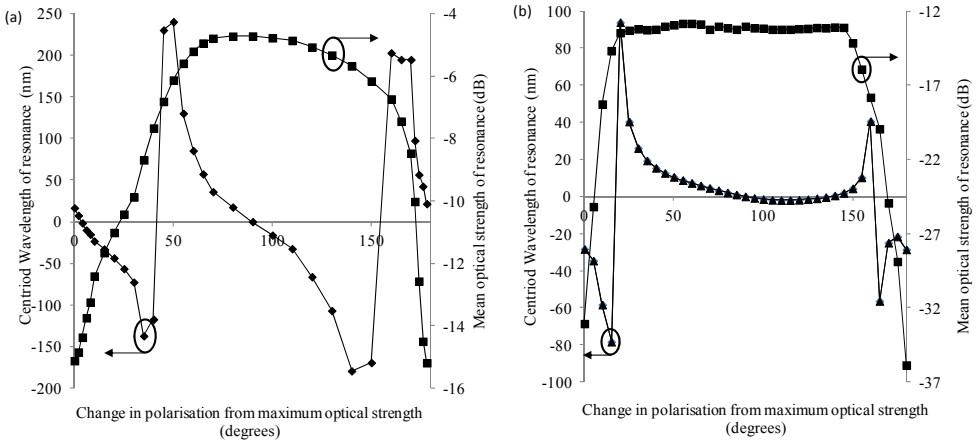

Fig. 10. The variation in central wavelength and coupling efficiency of the SPR as a function of change of polarization azimuth at the polarization controller. The angle is measured from the point of maximum coupling strength. The data relate to an Au-SiO_2-Ge coated device (a) before (1370nm center of spectral feature) and (b) after UV processing (1350nm center of spectral feature)

Table 1. A summary of the spectral behavior of the surface plasmon resonance fiber devices as a function of azimuthal polarization of the illuminating light.

Metal overlay	UV	Wavelength tunability (nm)	Azimuthal polarization range (degree)	Peak optical strength (dB)	Mean optical strength (dB)
Platinum	Before	400	50	31	6
	After	250	35	48	10
Gold	Before	400	60	15	5
	After	200	20	36	12
Silver	Before	140	65	22	5
	After	70	40	33	8

In addition some modelling was performed, calculating the expected phase matching of the LSP a as function of surrounding refractive index. This was achieved by using the FFT of

#189539 - $15.00 USD Received 30 Apr 2013; revised 14 Jul 2013; accepted 21 Jul 2013; published 31 Jul 2013

the measured surface topology of the device obtained using AFM to determine the lattice constants for the calculations to predict the spectral response of the LSP [24]. We have assumed that there is coupling between the $HE_{1,1}$ and higher order modes to several localized surface plasmons with scattering integer order $i = 1$ for the dominant periods found in the FFT in the region 0.18 μm to 0.98 μm. The modelling generated excitation resonances that reasonably matched the experimental data. The authors would like to state that there are more modes with the correct phase matching condition in this spectral range but the experimental results suggest only a few of these modes have a significant coupling to the surface plasmons, otherwise very broadband losses would be observed experimentally. Predicting these coupling strengths for each mode is a work-in-progress. The modeling is used here to predict spectral location and spectral response of plasmons to changes in refractive index using a similar procedure to [13]. The theoretical results are shown in Fig. 11(a) for a platinum metal overlay with corresponding experimental results shown in Fig. 8. The same modelling approach has also been used for another fabricated LSP fiber device (Ag metal overlay coating) which has different dominant periods in the coating structure, see Fig. 11(b), and was found to display reasonable agreement with experimental data and. This plot also demonstrates that for different metallic overlay, different spectral behavior can occur [13].

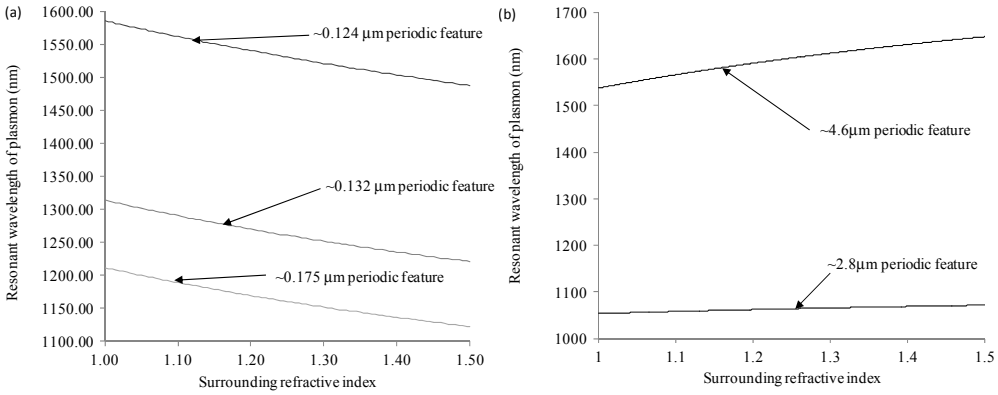

Fig. 11. (a) The theoretically predicted - surface plasmon resonances condition as a function of refractive index for a Pt-SiO_2-Ge coated device with the spatial lattices given by the FFT of Fig. 8 and with the scattering integer order ($i = 1$). This is only showing the coupling with the $HE_{1,1}$ mode. (b) Another example of LSP device, Ag-SiO_2-Ge coated.

3. Conclusion

It has been shown that conventional metal coated SPR optical fiber sensors based upon either long range or damped surface plasmons can be transformed into localized surface plasmons using a relatively uncomplicated procedure using UV laser irradiation and a phase mask designed for the purpose of inscribing Bragg gratings into optical fiber. Evidence is presented that shows that regardless of the metal overlay in the multi-layered coating, there is an optimum UV dosage of approximately 48 joules over which no significant additional optical change is observed. This suggests that the germanium and silicon dioxide are the dominant factors in the coupling of the light to the surface of the fiber and thus to the surface plasmons.

This fabrication method can produce a nano-scaled surface relief grating structure that resembles an array of nano-wires with an individual nano-wire having typical dimensions of width of 100nm and length of 20μm. Experimental data have been presented that show changes in spectral characteristics after UV processing and that the overall sensing performance of these sensors increases significantly from that of its pre-UV exposure state. Furthermore, polarization properties were studied before and after UV processing, which showed dramatic changes in spectral behavior with increased sensitivity to polarization, along with a smaller tuning wavelength range of as a function of azimuthal polarization state for a given SPR excitation. This spectral behavior is consistent with nano-rod behavior as a

#189539 - $15.00 USD Received 30 Apr 2013; revised 14 Jul 2013; accepted 21 Jul 2013; published 31 Jul 2013

function of polarization. More individual plasmon resonances are observed after UV processing; this is expected from theoretical predictions using the predominant periods that exist within the coating (on the fiber) and reasonable agreement was found with experimental data. It has been shown that these devices can generate surface plasmons over a very large wavelength range, (visible to 2 μm) depending on the azimuthal polarization state of the illuminating light. The transformation of the SPR to LSP fiber devices by UV processing enhances their spectral sensitivity to changes in the surrounding environment's refractive index, such as was observed with the Ag-SiO2-Ge device, which yielded the highest spectral sensitivity in the aqueous index regime of 4000 nm/RIU for wavelength and 800 dB/RIU for intensity.

Acknowledgments

This work is funded by EPSRC Joint Research Grant: EP/J010413/1 Title: Grating and waveguide plasmonic sensors. Also we would like to acknowledge that some funding came from European Regional Development Fund (CEITEC-CZ.1.05/1.1.00/02.0068) and the EU 7th Framework Programme (SYLICA and 280566 - UnivSEM)

#189539 - $15.00 USD Received 30 Apr 2013; revised 14 Jul 2013; accepted 21 Jul 2013; published 31 Jul 2013